

Dynamic model of ex vivo granulocytic kinetics to examine the effects of oxygen tension, pH, and interleukin-3

Diane L. Hevehan, Larissa A. Wenning, William M. Miller, and E. Terry Papoutsakis

Department of Chemical Engineering, Northwestern University, Evanston, Ill., USA

(Received 4 February 2000; revised 24 April 2000; accepted 28 April 2000)

Objective. Evaluating kinetics in hematopoietic cultures is complicated by the distribution of cells over various stages of differentiation and by the presence of cells from different lineages. Thus, an observed response is an integral response from distributed cell populations. Growth factors and other parameters can greatly affect the lineage and maturation stage of the culture outcome. To resolve the kinetics and more clearly define the differential effects of O₂ tension (pO₂), pH, and interleukin-3 (IL-3) on granulopoiesis, a mathematical model-based approach was undertaken.

Materials and Methods. Granulocytic differentiation is described within a continuous, deterministic framework in which cells develop from primitive granulocytic progenitors to mature neutrophils. The model predicts two distributed populations—quiescent and cycling cells—by incorporating rates of growth, death, differentiation, and transition between quiescence and active cycling. The response of these four model processes to changes in the culture environment was examined.

Results. Model simulations of experimental data revealed the following: 1) pO₂ effects are exerted only on the growth rate but not maturation times. 2) pH effects between pH 7.25 and 7.4 on growth and differentiation are coupled; however, with increasing pH values, especially at pH 7.6, the death rate for cells in the early stages of differentiation becomes increasingly significant. 3) The absence of IL-3 increases the death rate for primitive cells only minimally but markedly enhances the rate of differentiation through the myeloblast window in the differentiation pathway. The combined effects of these environmental factors can be predicted based on changes in the model parameters derived from the individual effects.

Conclusions. Experimental data combined with mathematical modeling can elucidate the mechanisms underlying the regulation of granulopoiesis by pO₂, pH, and IL-3. The model also can be readily adapted to evaluate the effects of other culture conditions. The increased understanding of experimental results gained with this approach can be used to modify culture conditions to optimize ex vivo production of neutrophil precursors. © 2000 International Society for Experimental Hematology. Published by Elsevier Science Inc.

Keywords: Mathematical model—Granulopoiesis—Oxygen tension—pH—Interleukin-3

Introduction

The 120 billion neutrophils, with a limited lifespan of only 48 hours, produced each day in a healthy adult form the first line of defense against microbial invasion. Maintaining or adjusting steady-state levels of neutrophils is dependent on the kinetic patterns of proliferation, differentiation, and death of granulocytic precursor cells that reside in the bone

marrow. Based on morphologic or flow cytometric criteria, these cells can be classified into six relatively distinct stages of maturation [1,2]. The first three stages comprising the sequence of granulocytic differentiation include proliferating myeloblasts, promyelocytes, and myelocytes. Later myeloid stages, i.e., metamyelocytes, band form neutrophils, and segmented neutrophils, can no longer divide, but they still continue to differentiate. The balance among proliferation, differentiation, and death of each granulocytic subpopulation is tightly regulated by complex interactions with growth and other regulatory factors. Specifically, O₂ tension (pO₂) and pH, in synergy with cytokines, contribute to this regulatory network by establishing distinct hematopoietic-

Offprint requests to: E. Terry Papoutsakis, Ph.D., Chemical Engineering Department, Northwestern University, 2145 Sheridan Road, Evanston, IL 60208-3120; E-mail: e-paps@northwestern.edu

Dr. Wenning is now with Merck Research Laboratories in West Point, Pa., USA.

inducing microenvironments. Results from our laboratory previously demonstrated the differential sensitivity of the various classes of hematopoietic cells to pO_2 , pH, and cytokines [3–8]. Not only may these factors act preferentially on one specific lineage, they may further elicit responses from cells occupying a distinct stage of differentiation.

We identified low pO_2 (5% O_2) and low pH (7.1–7.25) as the optimal culture conditions for producing cells of the granulocytic lineage, especially in the postprogenitor stages of development [8]. The experimental data suggested that pO_2 was affecting only cell proliferation, whereas pH seemed to influence both proliferation and differentiation. The roles of several growth factors, including those of interleukin-3 (IL-3), in regulating a large number of distinct biologic processes have been well-characterized. Of particular relevance to optimizing granulocytic cell production are IL-3's pleiotropic activities in stimulating the proliferation, survival, and differentiation of multipotent progenitor cells and granulocyte lineage-committed cells [9–13].

When cells are exposed to suboptimal pO_2 or pH conditions or to limited amounts of IL-3, cell death may occur, proliferative cells might fail to divide, or progenitor cells might alter their rate of differentiation. Discriminating between these possibilities based on direct observation is hindered, in part, by the complex culture behavior, i.e., the distribution of cells at various stages of differentiation and/or the presence of cells of other lineages. Regulation of granulocytic cell production by pO_2 , pH, and IL-3 is incompletely understood, especially regarding its quantitative aspects. Key questions include the following: 1) What processes—proliferation, differentiation, death, and/or transition between quiescence and active cycling—contribute to the observed differences in cell numbers? 2) Are these effects restricted to only specific stages of differentiation, or are they observed uniformly along the whole granulocytic differentiation pathway? 3) What are the magnitudes of these effects?

The aim of the present study was to address these questions by establishing and applying a model-based approach to deconvolute selected environmental (pO_2 , pH, and IL-3) effects on the dynamic properties of the granulopoietic system as a whole. Previous mathematical models of human granulopoiesis that compartmentalize cells in discrete stages make certain nonphysiologic assumptions and ignore the range in expansion potential within each designated stage [14,15]. As an improvement on these earlier models, we propose here that the highly dynamic granulopoietic system can be described as a continuous, deterministic process from lineage-committed progenitor cells to mature neutrophils. Analogous to a previously developed framework for erythropoiesis [16], each stage of granulocytic differentiation (colony-forming unit granulocyte [CFU-G], myeloblasts, promyelocytes, myelocytes, metamyelocytes, bands, and segmented granulocytes) represents a fraction of the total differentiation process based on experimental observation. Model simulations yield distributed populations of

active, quiescent, and mature cells. Experimentally, granulocytic proliferation, differentiation, and death patterns under different culture conditions and as a function of time were characterized by total cell concentration, viability, colony-forming cell (CFC) content, cell-surface marker staining (CD15/CD11b), and annexin V staining.

In addition to providing a conceptual framework within which one can elucidate the mechanisms underlying the environmental regulation of granulopoiesis, integration of cell culture experiments with mathematical modeling is a valuable tool for improving ex vivo culture strategies. Ex vivo expansion of mobilized peripheral blood CD34⁺ cells along the granulocytic lineage has potential applications for ameliorating neutropenia after high-dose chemotherapy [17–21]. By mathematical modeling, it is possible to better interpret experimental results and to modify the culture conditions to obtain the desired output at an optimal harvest time.

Materials and methods

Experimental methods

Culture setup. The experimental design and methods were described previously [8]. Briefly, mobilized peripheral blood CD34⁺ cells selected 48 hours after collection were seeded at 2×10^4 cells/mL and cultured for 13 to 15 days in serum-containing medium supplemented with 50 ng/mL recombinant stem cell factor (SCF; Amgen, Thousand Oaks, CA), 10 ng/mL recombinant IL-6 (Peprotech, Rocky Hill, NJ), and 10 ng/mL recombinant granulocyte colony-stimulating factor (G-CSF; Amgen) in the presence or absence of 10 ng/mL recombinant IL-3 (R&D Systems, Minneapolis, MN). An additional 10 ng/mL G-CSF was added to the cultures every 2 days to compensate for its depletion due to degradation at 37°C. Cultures were fed by dilution with fresh medium containing growth factor to maintain densities between 7.5×10^4 and 2.5×10^5 cells/mL. Different culture conditions were imposed by adjusting the pH of the media with the addition of a predetermined volume of sterile 1N HCl or 1N NaOH and equilibration in a fully humidified atmosphere of either 5% O_2 , 5% CO_2 , and balance N_2 , or air and 5% CO_2 . Beginning on day 2 or 3 and every odd day thereafter, cultures were assessed for total cell concentration using a Coulter Multisizer, cell viability using trypan blue dye, progenitor cell content using a CFC assay, and cellular phenotype by flow cytometric staining for CD15 and CD11b. Data for the seven conditions, each evaluated in cultures from six to seven different patient samples (Response Oncology, Memphis, TN), were used for modeling purposes: 5% O_2 , pH 7.6, +IL-3; 5% O_2 , pH 7.4, +IL-3; 5% O_2 , pH 7.25, +IL-3; 20% O_2 , pH 7.4, +IL-3; 20% O_2 , pH 7.25, +IL-3; 5% O_2 , pH 7.4, -IL-3; and 5% O_2 , pH 7.25, -IL-3. The environment of 5% O_2 , pH 7.25, +IL-3 was designated as the “control” condition because it was the least inhibited condition among those examined for the production of granulocytic cells.

Flow cytometry. Cellular phenotype. Day 0 and cultured cells were evaluated for expression of the granulocyte lineage-associated antigens CD15 and CD11b. Standard flow cytometric techniques were used and are described in detail elsewhere [8].

Apoptosis. Cultures were monitored for apoptosis every 3 hours during the first 12 hours of culture and then at increasingly longer

intervals thereafter, using the annexin V flow cytometric assay. The annexin V-fluorescein isothiocyanate (FITC) staining protocol and reagent preparation were carried out according to recommendations by the manufacturer (Pharmingen, San Diego, CA). Briefly, 1×10^5 cells were washed twice with phosphate-buffered saline (10 mM, pH 7.4) and resuspended to a concentration of 1×10^6 cells/mL in $1 \times$ binding buffer—a buffer containing Ca^{2+} , which is required for annexin V to bind to exposed phosphatidylserine residues. Five microliters of annexin V-FITC and $10 \mu\text{L}$ of propidium iodide $50 \mu\text{g/mL}$ were added, and the mixture was incubated at room temperature in the dark. After 20 minutes, the sample was diluted with $400 \mu\text{L}$ of $1 \times$ binding buffer and immediately analyzed on a FACScan flow cytometer (Becton-Dickinson, San Jose, CA). Additional control tubes to compensate for fluorescence spectral overlap were prepared as necessary.

Modeling methods

Conceptual structure of the model. Stem cells determined for granulopoiesis go through several mitoses, commit to differentiation, and finally mature into morphologically recognizable granulocytic progenitors. Following lineage commitment, extensive expansion and maturation take place. CFU-G represents the first lineage-specific stage of granulopoiesis. These granulocytic progenitors divide several times, thus amplifying cell numbers, and differentiate into myeloblasts, promyelocytes, and then myelocytes [2,22]. A single granulocytic progenitor may undergo a maximum of approximately 17 divisions [23]. Beginning at the myelocyte to metamyelocyte stage, cells lose the capability to divide, but they continue to differentiate until they reach terminal maturation as mature neutrophils [2,22]. Given that the *in vitro* cultures to be modeled consisted primarily of granulocytic cells, with only a small monocytic population that could be subtracted off, granulocytic differentiation was modeled as a continuous and deterministic, unilineage process (Fig. 1).

The net production of cells with time results from a combination of processes, such as division, maturation, and death, which may be occurring simultaneously. The dormancy vs cycling status of cells is an additional dimension that is included within the model to more accurately depict the *ex vivo* situation in which the culture kinetics during the first few days may be dominated by the transition from quiescence to active cycle. The model allows for the independent regulation of the rates of each of these cellular processes and, in particular, the decoupling of the rate of differentiation from the rate of cell division.

Mathematical structure of the model. Two distributed density populations that represent the quiescent and cycling populations are defined as functions of time (t) and τ : $n_0(t, \tau)$ and $n(t, \tau)$, respec-

tively. τ is a measure of the extent of differentiation with values ranging between 0 and 1. $\tau = 0$ corresponds to commitment of multipotent cells to the granulocytic lineage, and $\tau = 1$ corresponds to fully mature granulocytes. Cell population balances on the active, quiescent, and mature populations are derived from the general equation:

$$\left[\begin{array}{c} \text{Rate of accumulation of cells at} \\ \text{time } t \text{ that are at a differentiation stage} \\ \text{between } \tau \text{ and } \tau + d\tau \end{array} \right] = \left[\begin{array}{c} \text{Net rate of influx - efflux} \\ \text{of cells as they differentiate} \end{array} \right] + \left[\begin{array}{c} \text{Net rate of} \\ \text{cell generation} \end{array} \right].$$

The generation term accounts for cells transiting between quiescence and cycling, cells generated through division, and cells lost due to death. More specifically, for active cells:

$$\left[\frac{\partial n}{\partial t} \right] = \left[\frac{-\partial(vn)}{\partial \tau} \right] + [\alpha n_0 + (\mu - \delta - \beta)n] \quad (1)$$

where v is the rate of differentiation, μ is the specific growth rate, δ is the specific death rate, α is the specific rate of quiescent-to-active transition, and β is the specific rate of active-to-quiescent transition; all parameters are functions of both t and τ .

In defining the number of quiescent cells, growth, differentiation, and death rates can be excluded from the cell balance because quiescent cells are considered to be triple quiescent, i.e., they do not divide, differentiate, or die:

$$\left[\frac{\partial n_0}{\partial t} \right] = [\beta n - \alpha n_0] \quad (2)$$

The number of mature granulocytes at $\tau = 1$, i.e., those cells no longer differentiating, becomes only a function of t : $N_M(t, 1)$. Because mature cells are well beyond their transition into the cell cycle and are no longer proliferating, the cell population balance can be written as follows:

$$\left[\frac{dN_M}{dt} \right] = [v(t, 1)n(t, 1)] - [\delta_M N_M] \quad (3)$$

where δ_M is the specific death rate of mature cells in the terminal stage.

To solve these equations, the initial time distributions for quiescent and active cells and the initial number of cells in the terminal stage [$n_0(0, \tau)$, $n(0, \tau)$, and $N_M(0)$, respectively] must be specified (Appendix A-1). In addition, the boundary condition at $\tau = 0$ is required (Appendix A-1). The model is solved numerically using the method of lines [24]. Further details of the model and its original biomathematical formulation are presented in the Appendix and elsewhere [16].

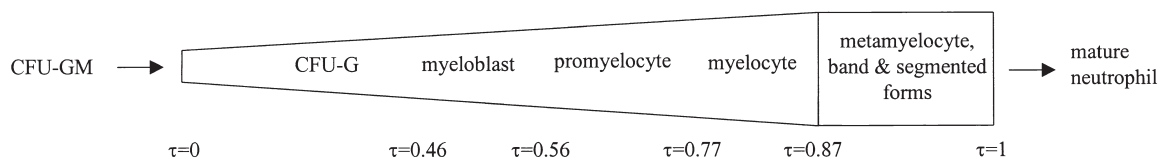


Figure 1. Schematic representation of the granulocyte differentiation pathway annotated with values of τ , a measure of the extent of differentiation (see text and Table 1 for details). Committed granulocytic progenitor cells, CFU-G ($0 < \tau < 0.46$), descend from bipotent progenitor cells, CFU-GM. Proliferating precursor cells consist of myeloblasts, promyelocytes, and myelocytes ($0.46 < \tau < 0.87$). Nonproliferating precursor cells, designated after the solid line, include metamyelocytes, bands, and segmented granulocytes ($0.87 < \tau < 1$).

Parameter estimation. Most values for the model parameters were derived from experimental data, such as cell counts and flow cytometric data. Others were adjusted until the model response provided good qualitative and quantitative fits to the data under the control conditions (5% O₂, pH 7.25, +IL-3), i.e., until the theoretical curves could reproduce experimental data within the error margins of the experiments. The best fit curves were determined by minimizing the sum of squares between the observed and predicted data. Although the experimental data were reproduced closely by the model, the values used for certain parameters on which the model analysis was based may not be generally valid. Some values may be particular to specific aspects of the culture system used. This must be considered when applying the model to new and independent types of experimental data.

To apply the proposed unilineage granulopoietic model, the true number of viable granulocytic cells observed experimentally was calculated by correcting the measured cell counts and cellular fractions for viability and the presence of any nongranulocytic cells. Under the influence of SCF, G-CSF, IL-6, and ±IL-3, cultures became predominantly granulocytic in nature but with a small population of up to 20% monocytic cells depending on the culture conditions. The fraction of monocytic postprogenitors could be easily quantified based on their distinct CD15/CD11b expression pattern. In contrast to granulocytic cells, which progress from CD15^{dim} to CD15^{bright} and finally to CD11b⁺, cells of the monocyte lineage first become CD11b⁺ and then acquire dim levels of CD15 [25], thus enabling us to subtract off the CD15⁻/CD11b⁺ and CD15^{dim}/CD11b⁺ monocytic populations.

Determining the initial number of granulocytic cells on day 0 and on the days before significant CD15^{bright} or CD11b expression, when CFCs predominate, required adjustment of total cloning efficiencies (CE; CFC/total cell). Total CEs typically were <20%, even on day 0, as detected by our standard colony assay; however, it is unlikely that >80% of the CD34⁺ cells die, remain dormant, or are either beyond or more primitive than the CFC stage. This suggests that the colony assay used was not a true indicator of proliferative potential. The frequency of hematopoietic progenitors arising from single CD34⁺ cells in liquid and methylcellulose cultures is a more accurate measure of CE, with values averaging ~55% based on reports in the literature for cultures evaluated at day 14 to 23 [23,26–29]. Thus, we scaled the observed day 0 total CE accordingly so that it reflects this value. Measured CE values on subsequent days were adjusted by the same ratio as on day 0 so that, although the absolute values for CE changed, the relative CFC kinetics remained the same.

Differentiation [τ and $\nu(t, \tau)$]. The extent of differentiation, designated as τ , was quantified using a scale from 0 to 1. The τ struc-

ture, with intervals corresponding to each differentiation stage, was deduced using the maximum proliferative capacity within the granulocytic lineage, together with our in vitro observations (Table 1 and Fig. 1). The most primitive CFU-G has the potential for 17 divisions according to a previous report by Mayani and Lansdorp [23]. The 17 divisions are distributed among the proliferative stages. The promyelocytes and myelocytes (CD15^{bright}/CD11b⁻ and CD15^{bright}/CD11b⁺, respectively), which no longer have colony-forming potential and do not express CD34, a progenitor cell-associated marker, may not undergo >6 divisions combined; otherwise, these cells would appear as CFU-G in colony assays. The remaining possible 11 divisions are divided among the CD15⁻/CD11b⁻ and CD15^{dim}/CD11b⁻ phenotypes, which retain the CD34 antigen ($n = 2$; data not shown). The finer divisions in τ were chosen based on our observed in vitro kinetics.

The transit time through each of the proliferative stages is calculated as the product of the assigned number of divisions and the constant 24-hour doubling time (t_d ; see section on “Specific growth rate”) that was observed in our control culture (Table 1). A maturation time of 60 hours was used for the nonproliferating cells—an estimate that is consistent with experimental findings [30,31]. Our data suggest that the model response does not depend significantly on the value chosen for the nonproliferative maturation time, because few cells in this study reached the very late differentiation stages and these cells were no longer dividing. The transit time through each individual stage normalized to the overall maturation time results in the τ structure presented in Figure 1 and Table 1. The total time it would take the most primitive CFU-G to fully mature is used to determine the corresponding differentiation rate $\nu(t, \tau)$. Under control conditions, $\nu(t, \tau)$ equals 1 differentiation unit per 468 hours and is assumed constant for all τ .

Specific growth rate (μ). $\mu (= \ln 2/t_d)$ is determined from data obtained between days 3 and 13 of our cultures, when most cells are active and proliferating. Within this time frame, t_d under control conditions is 24 hours. It was shown that t_d may vary with differentiation stage [32]. However, although the model provides for a distributed growth rate function $\mu(t, \tau)$, the data can be well approximated by a constant growth rate $\mu(t, \tau) = \ln 2/24$ for all the proliferative stages, i.e., CFU-G, myeloblast, promyelocyte, and myelocyte. The slower rate of increase in cell numbers after day 13 is consistent with the increasing number of cells entering the nonproliferative stages, from metamyelocyte to neutrophil. For nonproliferating granulocytes ($0.87 < \tau < 1$), $\mu = 0$.

Specific death rates (δ and δ_M). We assume that in our control culture under optimal stimulation (5% O₂, pH 7.25 with SCF, G-CSF, IL-6, and IL-3), the rate of granulocytic cell death at each stage is 0, i.e., $\delta(t, \tau) = \delta_M(t) = 0$. This is consistent with the negli-

Table 1. Normalization of granulocyte differentiation using a τ structure to represent the fraction of time it takes a cell to progress through each differentiation stage

Differentiation stage	Phenotype	Max Divisions	Stage duration (h)	τ
CFU-G	CD15 ⁻ /CD11b ⁻	9	216	$0 < \tau < 0.46$
Myeloblasts	CD15 ^{dim} /CD11b ⁻	2	48	$0.46 < \tau < 0.56$
Promyelocytes	CD15 ^{bright} /CD11b ⁻	4	96	$0.56 < \tau < 0.77$
Myelocytes	CD15 ^{bright} /CD11b ⁺	2	48	$0.77 < \tau < 0.87$
Metamyelocytes, bands	CD15 ^{bright} /CD11b ⁺	0	60	$0.87 < \tau < 1$
Total		17	468	$0 < \tau < 1$

Values are based on a constant doubling time of 24 h under maximal stimulation (control conditions: 5% O₂, pH 7.25, +IL-3). See text for details.

Table 2. Response of model parameters to environmental changes

Culture condition	$t_d (\pm \% \Delta t_d)^\dagger$ $0 < \tau < 0.87$	$\nu (\pm \% \Delta \nu)$ $0 < \tau < 1$	$\langle \overline{\nu/\mu} \rangle^\ddagger$ $0 < \tau < 0.87$	δ $0 < \tau < 0.25$
5% O ₂ , pH 7.25, +IL-3*	24 h	1/468 h ⁻¹	0.074	0 h ⁻¹
5% O ₂ , pH 7.4, +IL-3	26 (8%)	0.9 × 1/468 (-10%)	0.072	0.01
5% O ₂ , pH 7.6, +IL-3	31 (29%)	0.9 × 1/468 (-10%)	0.086	0.04
20% O ₂ , pH 7.25, +IL-3	27.5 (15%)	1/468 (0%)	0.085	0
20% O ₂ , pH 7.4, +IL-3	30.5 (27%)	0.9 × 1/468 (-10%)	0.085	0.01
5% O ₂ , pH 7.25, -IL-3	29 (21%)	0 < τ < 0.46: 1/468 (0%) 0.46 < τ < 0.56: 3.3 × 1/468 (+230%) 0.56 < τ < 1: 0.8 × 1/468 (-20%)	0.107	0.005
5% O ₂ , pH 7.4, -IL-3	34 (42%)	0 < τ < 0.46: 0.9 × 1/468 (-10%) 0.46 < τ < 0.56: 3 × 1/468 (+200%) 0.56 < τ < 1: 0.6 × 1/468 (-40%)	0.108	0.015

*Control condition.

†Parenthetic values refer to the percent increase (+) or decrease (-) from the value at the control condition.

‡ $\mu = \ln 2/t_d$.

gible amount of apoptosis observed throughout cultures under these conditions (Fig. 3), high viabilities, and the fact that the combination of four cytokines used in these experiments is known to attenuate cell death and enhance granulopoiesis [33,34]. Furthermore, because only a minor fraction of cells actually matured to $\tau = 1$ by the end of the culture period (16% under control conditions), it is unlikely that the cells reached the end of their natural lifespan during the culture period. The model does, however, allow the incorporation of a variable death rate because the probability of cell death may increase under suboptimal conditions, e.g., higher pH (see Results).

Specific transition rates (α and β). Early culture kinetics are likely to be dominated by the transition from quiescence to active cycling. Pregranulocytic cells that have a greater tendency to remain quiescent were rare events. Therefore, the transition into cycling is assumed to occur at a constant rate α , which is independent of the degree of differentiation τ . α was determined to be 0.10 h⁻¹ based on a qualitative fit of total cell numbers observed during the first 3 days of culture at the control conditions. In a cytokine-rich environment, cells are unlikely to revert to quiescence after the initial transition into the active cycle and, thus, β can be neglected.

Model representation of observed granulocytic cell types. Model outputs of the populations $n(t, \tau)$, $n_0(t, \tau)$, and $N_M(t)$ can be related to an observed quantity, $O(t)$, through the integral equation:

$$O(t) = \int_{\tau=0}^1 w_0(\tau)n_0(t, \tau)d\tau + \int_{\tau=0}^1 w(\tau)n(t, \tau)d\tau + w_M N_M(t). \quad (4)$$

Assigning a weighting function $w(\tau)$ to each differentiation marker results in a set of similar equations describing each of the different granulocytic cell types—CD15⁺, CD15^{bright}, CD11b⁺, and total cells (Appendix A-2).

Results

Figures 2 and 4–6 show model simulations of the kinetics of granulopoiesis observed in cultures at different O₂ tensions,

pH values, and in the presence or absence of IL-3. Time profiles are given for the production of the total number of granulocytic cells and the percentages of each granulocytic cell subpopulation. The three differentiation curves represent the progression of granulocytic maturation as cells first acquire the CD15 antigen at low levels on the cell surface (CD15^{dim}), then at greater levels (CD15^{bright}), and finally as they acquire CD11b. Experimental data points represent mean values from at least six different patient samples. Baseline values of the cell kinetic parameters— μ , ν , δ , β , and α —were derived from control cultures at 5% O₂, pH 7.25, +IL-3, the most favorable conditions for granulocytic cell production (Table 2). Fitting the model to data for other conditions involved 1) adjusting a minimum number of parameters and 2) making these changes across all τ or, if necessary, only for an isolated range of τ . Model analysis showed that α remains constant at 0.10 h⁻¹ under all conditions tested, indicating no adverse effects on the induction of cycling. Considering this, and that β could be neglected (see section on “Parameter estimation”), the potential effects of pO₂, pH, and IL-3 were reflected in the remaining three parameters. The model parameters for each case and the relative changes in these values compared to the control cultures are summarized in Table 2. The ν/μ ratio averaged over $0 < \tau < 0.87$, $\langle \overline{\nu/\mu} \rangle$, serves as a means to compare the balance between differentiation and proliferation. When comparing two culture conditions, a constant $\langle \overline{\nu/\mu} \rangle$ indicates that the effects exerted on differentiation and proliferation are coupled.

Model simulation of pO₂ effects:

5% O₂ vs 20% O₂ (pH 7.25, +IL-3)

The experimental curves showed that total, CD15^{bright}/CD11b⁻, and CD15^{bright}/CD11b⁺ cell expansion is enhanced at 5% O₂ relative to that at 20% O₂ [8]. The effects of O₂ on cell numbers gradually increased throughout culture, but patterns of differentiation appeared markedly similar.

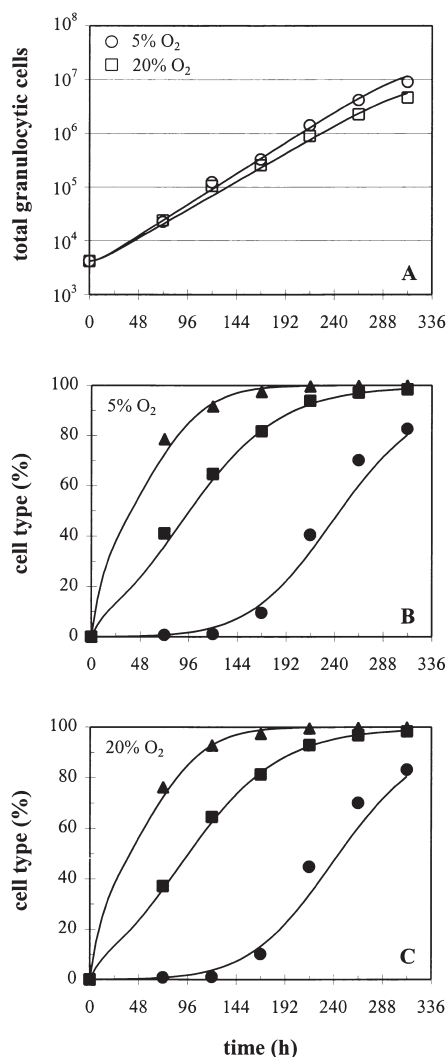


Figure 2. Effects of pO₂ on the kinetics of granulocytic cell production and differentiation. Model simulations (—) are compared to experimentally observed values for total granulocytic cell numbers (A) and percentages of CD15⁺ (▲), CD15^{bright} (■), and CD11b⁺ (●) cells as a function of time in cultures under 5% O₂ (B) or 20% O₂ (C), both at pH 7.25 and in IL-3-containing media. Culture behavior was simulated using the model parameters listed in Table 2.

In the model, increasing the doubling time (t_d) by 10%, for cultures under 20% O₂, relative to 5% O₂ at pH 7.25, was found to reproduce the twofold decrease in total granulocytic cell numbers without disturbing the fractions of each subpopulation (Fig. 2). The longer t_d (slower growth rate, μ) at 20% O₂ with the same differentiation rate (ν) results in an increase in $\langle \bar{\nu}/\bar{\mu} \rangle$ (Table 2). This increase means that cells cultured at the higher pO₂ will divide less (by one mitosis) by the time they reach $\tau = 0.87$. Achieving a reasonable fit with a single modification in t_d indicates, and is consistent with experimental findings [8], that the effects of pO₂ are isolated to the proliferation process and that these effects are not coupled with differentiation.

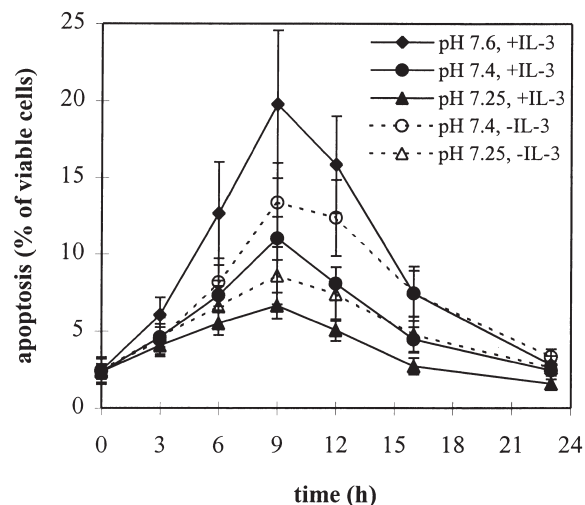


Figure 3. Percentage of viable cells that undergo apoptosis within the first 24 hours of culture at the indicated conditions. Apoptosis was measured via flow cytometric detection of annexin V binding. Peak values were obtained 9 hours after culture initiation with increases over control conditions (5% O₂, pH 7.25, +IL-3; $n = 5$) as follows: 197% at 5% O₂, pH 7.6, +IL-3 ($n = 3$); 101% at 5% O₂, pH 7.4, -IL-3 ($n = 3$); 66% at 5% O₂, pH 7.4, +IL-3 ($n = 5$); and 29% at 5% O₂, pH 7.25, -IL-3 ($n = 3$). There was no difference in the extent of apoptosis at any time in cultures under 20% O₂ relative to cultures under 5% O₂ at the corresponding pH in IL-3-containing media (data not shown; $n = 2$).

Model simulation of pH effects:

pH 7.4 and 7.6 vs pH 7.25 (5% O₂, +IL-3)

The experimental curves for cultures at pH 7.4 and pH 7.6 display two characteristics: decreased cell expansion concomitant with a reduced differentiation rate compared to cultures at pH 7.25. Unlike the case for pO₂, comparison with experimental data clearly indicates that changes in growth rates alone are not sufficient to reproduce the measured granulocytic response to pH [8]. After accounting for the increased fraction of monocytic cells—reaching maximum levels of 20% on days 7 to 9 at pH 7.6—the granulocytic differentiation profiles at pH 7.6 and 7.4 were identical to each other but were delayed compared to those at pH 7.25. Combining longer doubling times with a slower overall differentiation rate (by 10%) for cultures at pH 7.4 and 7.6, as suggested by previously shown experimental results [8], provided an adequate fit but could not reproduce the more rapid rise in the fraction of cells first acquiring CD15 that was observed at higher pH and was most pronounced at pH 7.6.

Acceleration of only the CD15⁺ curve during the first 3 days of culture at higher pH values results from a reduced percentage of CD15⁻/CD11b⁻ cells and indicates that either some fraction of cells are dying after leaving quiescence or cells are differentiating faster from the CD15⁻/CD11b⁻ to the CD15^{dim}/CD11b⁻ stage. Because previous experimental data could not discriminate between the two possibilities, we examined the extent of apoptosis during cultures at dif-

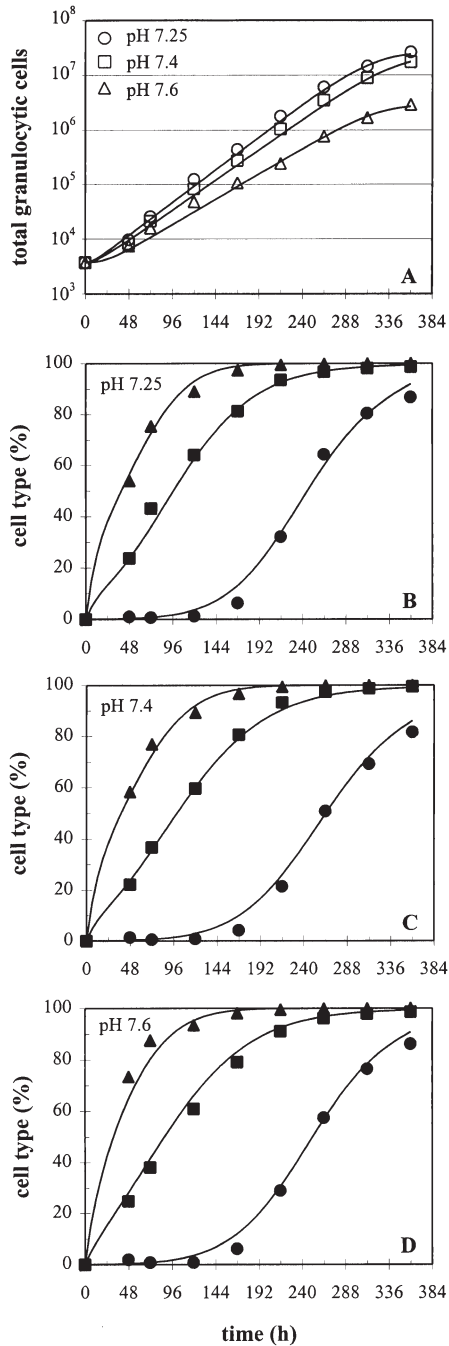


Figure 4. Effects of pH on the kinetics of granulocytic cell production and differentiation. Model simulations (—) are compared to experimentally observed values for total granulocytic cell numbers (A) and percentages of CD15⁺ (▲), CD15^{bright} (■), and CD11b⁺ (●) cells as a function of time in cultures at pH 7.25 (B), pH 7.4 (C), or pH 7.6 (D), all under 5% O₂ and in IL-3-containing media. The model parameters used to simulate the culture behavior at each pH are listed in Table 2.

ferent pH values (Fig. 3). The fraction of viable cells that were apoptotic peaked 9 hours after culture initiation, decreased to <2% by 24 hours, and remained at low levels for the duration of culture. Apoptosis was found to be more

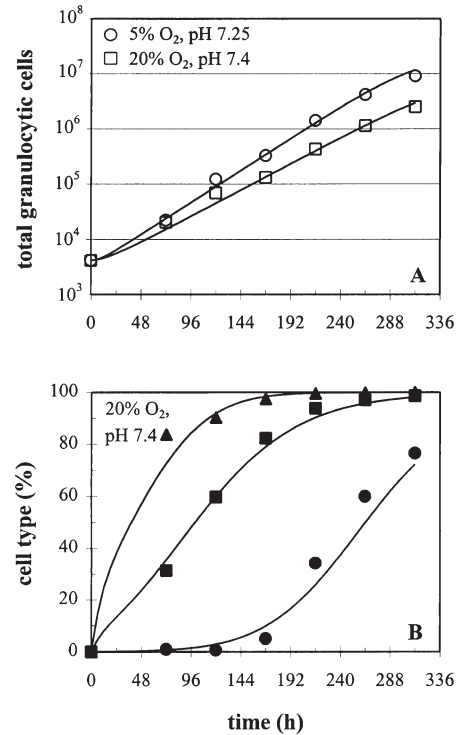


Figure 5. Combined effects of pO₂ and pH on the kinetics of granulocytic cell production and differentiation. Model simulations (—) are compared to observed values for total granulocytic cell numbers (A) and percentages of CD15⁺ (▲), CD15^{bright} (■), and CD11b⁺ (●) cells as a function of time in cultures at 20% O₂ and pH 7.4 (B) in IL-3-containing media. Model predictions of culture behavior were based on the parameters listed in Table 2. Note that the experimental data and model simulation for total granulocytic cell numbers produced under control conditions are provided for comparison (A).

prevalent in cultures at greater pH. There was a 66% and a 197% increase in the peak apoptotic fraction for cells at pH 7.4 and 7.6, respectively, over that for cells at pH 7.25. An elevated number of dead (PI⁺) cells at greater pH during the first few days of culture also was noted (data not shown). Based on this experimental evidence, a small, but finite, death rate that increases as pH increases and is restricted to only primitive cells was introduced into the model. Defining the cell loss in cultures at pH 7.4 or 7.6 with a relative death rate (δ) of 0.01 h⁻¹ or 0.04 h⁻¹, respectively, for 0 < τ < 0.25, combined with an altered t_d and ν , best captures the culture kinetics of the early stages of differentiation (CD15⁺) without affecting the fractions of subsequent granulocytic subpopulations (Fig. 4).

The model indicates that the effects of pH between pH 7.25 and 7.4 on growth and differentiation are coupled. The constant $\langle \bar{\nu}/\bar{\mu} \rangle$ value between cultures at pH 7.25 and 7.4 illustrates that although t_d is longer (μ is slower) at pH 7.4, there is a corresponding slower ν (Table 2). Thus, a maximum of 17 divisions would still be possible at pH 7.4 given enough time for cells to fully differentiate. Similar levels of cell production would be expected for cultures at pH 7.4 and

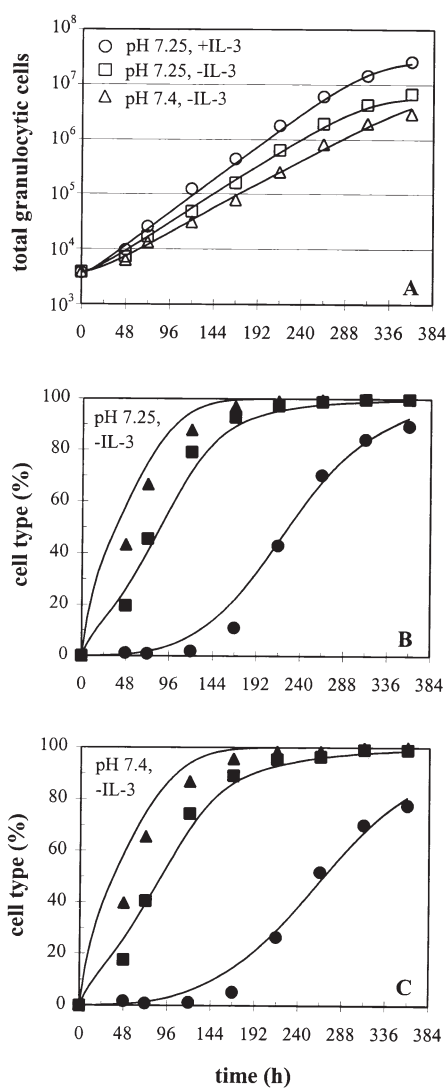


Figure 6. Effects of IL-3, independent of and combined with pH effects, on granulocytic kinetics. Model simulations (—) are compared to experimentally observed values for total granulocytic cell numbers (A) and percentages of CD15⁺ (▲), CD15^{bright} (■), and CD11b⁺ (●) cells as a function of time in cultures without IL-3 at pH 7.25 (B) or at pH 7.4 (C), both under 5% O₂. Culture behavior was simulated using the model parameters listed in Table 2. Note that the experimental data and model simulation for total granulocytic cell numbers produced under control conditions are provided for comparison (A).

7.25, but with slightly fewer cells due to a minimal amount of apoptosis at pH 7.4 during the earliest proliferative stage. However, no further slowing in ν occurred between pH 7.6 and 7.4 to counterbalance the even longer t_d at pH 7.6. The resulting increase in $\langle \overline{\nu/\mu} \rangle$ at pH 7.6 (Table 2) indicates that it is not possible to achieve the same number of divisions as obtained at pH 7.25 or 7.4. The lack of cell expansion at pH 7.6 also can be attributed in part to more extensive apoptosis at low τ as the pH increases.

With a separate, independent set of data that compared cultures at pH 7.25 and 7.4 [8], similar relative changes in

the model parameters were obtained, although the absolute growth rates differed due to patient-to-patient variability (simulations not shown).

Model simulation of combined pO₂ and pH effects:

20% O₂ and pH 7.4 (+IL-3)

The inhibitory effects of culturing cells under 20% O₂ or at pH 7.4 were cumulative for cells cultured simultaneously under 20% O₂ and pH 7.4 [8]. Simulation of the experimental time courses for cultures at 20% O₂ and pH 7.4 was achieved by addition of the changes in the kinetic parameters μ , ν , and δ that were derived from values obtained by model analysis of the individual effects of pO₂ or pH (Table 2 and Fig. 5). Preservation of the pO₂ effect, independent of pH, was indicated by the increase in $\langle \overline{\nu/\mu} \rangle$ at 20% O₂ vs 5% O₂ at pH 7.4, which was of the same magnitude as the increase at 20% O₂ vs 5% O₂ at pH 7.25 (Table 2). Furthermore, the pH effects were upheld regardless of pO₂, with $\langle \overline{\nu/\mu} \rangle$ remaining constant between pH 7.25 and pH 7.4 (Table 2). Maintenance of the individual effects on the model parameters under combined conditions indicates that pO₂ and pH are independently regulating different aspects of granulopoiesis and demonstrates the predictive capability of the model.

Model simulation of IL-3 effects:

–IL-3 vs +IL-3 (5% O₂, pH 7.25)

The absence of IL-3 during culture drastically reduced cell expansion, with 71% less total granulocyte production in –IL-3 cultures than that in +IL-3 cultures at 5% O₂, pH 7.25. The sensitivity of cells to apoptosis early on in culture increased by 29% compared to control conditions (Fig. 3). The effects on cellular differentiation appeared to be restricted to only an intermediate period during which cells cultured in the absence of IL-3 more rapidly pass through the CD15^{dim}/CD11b[–] compartment and accumulate in the CD15^{bright}/CD11b[–] stage before acquiring CD11b.

As anticipated from the observed data, appropriate changes in t_d and δ (Table 2) while using the same constant ν as in the control +IL-3 culture (1/468 h^{–1}) provide a reasonable fit of the total, CD15⁺ and CD11b⁺ curves, but do not adequately capture the steepness of the CD15^{bright} curve. Defining a relative death rate or increasing the rate of differentiation at intermediate τ values could account for the acceleration of the CD15^{bright} curve in the absence of IL-3, similar to the treatment of the model at early τ to capture the acceleration of the CD15⁺ curve with increasing pH (see section on “Model simulation of pH effects”).

Isolating IL-3’s anti-apoptotic effects to a small window in the middle of the differentiation pathway seems contrary to its reported ability to prevent the death of multipotent progenitors [9,10]. We would expect that if IL-3’s anti-apoptotic effects were responsible for the observed behavior, cells in the earliest position in the progenitor hierarchy, i.e., at low values of τ , would be equally or more sensitive to its absence. Although a good fit is obtained for all experimen-

tal curves by providing for a small amount of death ($\delta = 0.01 \text{ h}^{-1}$) for $0.46 < \tau < 0.56$, extending this window of sensitivity to include earlier values of τ results in a poor fit of the data (not shown).

It is more likely that the differentiation rates vary with τ in $-IL-3$ cultures. Accelerating differentiation through the regulatory window $0.46 < \tau < 0.56$ (by 230%) (Table 2) is consistent with our observations and improves the fit of the $CD15^{\text{bright}}$ differentiation curve (Fig. 6). The increase in $\langle \overline{v/\mu} \rangle$ in $-IL-3$ cultures, compared to control conditions, signifies that the effects on differentiation are not commensurate with those on proliferation, resulting in a fewer number of possible divisions (Table 2).

Model simulation of combined IL-3 and pH effects:

pH 7.4 and $-IL-3$ (5% O_2)

The experimental curves illustrate that the adverse effects on growth, differentiation, and death when culturing cells in the absence of IL-3 were magnified at higher pH values. Total granulocytic cell production was 87% less in pH 7.4, $-IL-3$ cultures at 5% O_2 than that in control cultures. Inhibition of cell expansion at pH 7.6 reached levels too high to allow the kinetic characterization of these cultures. To simulate the combined effects of IL-3 and pH 7.4, the individual effects on each model parameter were considered. As in $-IL-3$ cultures at pH 7.25, a variable differentiation rate was used to reproduce the three differentiation curves. Initially, for $0 < \tau < 0.46$, cells differentiate at the same rate as in pH 7.4, $+IL-3$ cultures. The subsequent changes in ν are similar in magnitude and occur over the same ranges of τ as those occurring in pH 7.25, $-IL-3$ cultures, with an increase in ν for $0.46 < \tau < 0.56$ by 233% compared to the initial ν for these conditions. Because the percent increase in apoptosis for cells cultured either at pH 7.4 (66%) or in the absence of IL-3 (29%) over control conditions was approximately additive for cultures combining the two conditions (101%) (Fig. 3), δ was assigned a value of 0.015. With these adjustments in ν and δ , and $t_d = 34$ hours, the model is able to simulate the behavior of $-IL-3$ cultures at pH 7.4 (Fig. 6).

The value of $\langle \overline{v/\mu} \rangle$ at these conditions coincides with the value calculated for $-IL-3$ cultures at pH 7.25 (Table 2). This indicates that the coupled effects on differentiation and proliferation induced by pH were maintained in $-IL-3$ cultures. Furthermore, at either pH value, $\langle \overline{v/\mu} \rangle$ increased in $-IL-3$ cultures vs $+IL-3$ cultures by the same amount. Therefore, a similar reduction in the number of possible cellular divisions occurs in the absence of IL-3 at pH 7.4 as at pH 7.25. This suggests that IL-3 and pH regulate granulopoiesis through independent pathways and further illustrates the predictive power of the model.

Discussion

The current model improves on several earlier models proposed for different aspects of proliferation and differentia-

tion of hematopoietic cells and cell lines [14,15,35–37]. In efforts to simplify a model or facilitate parameter estimation, some models treated cellular processes as combined events, e.g., coupling proliferation and differentiation [37]. However, these processes may or may not be closely linked, depending on the environmental conditions. It has been well established that different cytokines control several facets of hematopoiesis and may independently regulate rates of growth and differentiation, as well as apoptosis and/or transition into or out of cycling. Similarly, it was anticipated based on our experimental observations that regulation by pH and pO_2 may involve only one or some combination of these processes [8]. Within the framework of the proposed mathematical model, the dynamics of granulocytic cell production are assumed to be governed by four processes: 1) growth, 2) differentiation, 3) death, and 4) the transition between quiescence and active cycling. An essential element of this model that allowed us to deconvolute the environmental effects on granulopoiesis is that each of the model parameters— μ , ν , δ , α and β —can be modified independently. With this provision, we were able to simulate not only the isolated effects of pO_2 , pH, or IL-3 on granulocytic kinetics but also predict the combined effects of these environmental parameters. Furthermore, the present model allowed us to clearly define whether the granulocytic-specific responses induced by these factors were dependent on the cells' maturation stage. Certain restrictions placed on the independent regulatory mechanisms, such as at the different levels of maturation, were needed to improve model behavior to reflect our experimental observations. Some of these restrictions had not been considered beforehand and led to unexpected conclusions that could not have been deduced using previously published models.

Low pO_2 was shown to be superior for production and maintenance of primitive colony-forming unit granulocyte-macrophage (CFU-GM) populations [3–5,38,39] and for production of neutrophil precursors in the postprogenitor stages of development [5,8]. Model analysis indicates that pO_2 effects on the proliferation process were not coupled with changes in other cellular processes and that this cellular response was not stage specific because all mitotically competent granulocytic cells were affected. Based on several reports suggesting that hematopoietic cells are susceptible to oxidative stress and damage at high pO_2 [40–44], we had expected that impaired granulocyte production at 20% O_2 was at least partly death controlled. Surprisingly, the extent of cell death did not vary with O_2 tension. Possible mechanisms responsible for the effects of pO_2 on granulopoiesis likely involve a change in humoral regulation that stimulates or inhibits cellular proliferation. G-CSF is the primary regulator of granulopoiesis and has profound effects on stimulating the proliferation of granulocytic precursors [45,46]. Although similar differentiation and G-CSF receptor (G-CSFR) expression patterns were observed under different O_2 tensions [8], this does not preclude a role for G-CSF/G-CSFR signaling. Reduced mitotic responsiveness at 20% O_2

could still be attributed to a defect in receptor/signal transduction that was not examined here.

In contrast to the effects of pO_2 on growth alone, the effects of pH on growth were linked to differentiation. Interestingly, the similar inhibition of growth and differentiation at pH 7.4, as revealed by the model, signifies an increase in cell division time with increasing pH levels. Thus, if cells are given enough time to fully differentiate, the same number of mitoses is possible at pH 7.4 as at pH 7.25. This fact was not obvious from the experimental data in which cultures frequently were ended while cells at pH 7.4 still retained some proliferative capacity. In contrast, it was deduced from the model that, given unlimited time, cultures at pH 7.6 still could not attain the same level of expansion as at lower pH values. Inefficient granulocytic cell production at pH 7.6 resulted in part from the greater loss of early progenitor cells (CFU-G) due to the heightened sensitivity of these cells to death. In the marrow, as cells leave the G_0 compartment, a fraction of them is lost presumably due to premature cell death for unknown reasons [47]. It is probable that this phenomenon is exacerbated by exposing cells to a nonphysiologic environment, such as pH 7.6. Cultures carried out at pH 7.6, although having little physiologic relevance, verified the observed trends in the kinetics of granulopoiesis with increasing pH and further tested the robustness of the model.

Among G-CSF's many functions is its ability to reduce the transit time of the proliferating cell stages [45,46]. It was determined from the model that higher pH values are associated with lengthening in the transit time (because of the longer cell division time), thus suggesting that the effects of pH are mediated through G-CSF. This is consistent with the inhibition of the increase in G-CSFR levels associated with maturation at pH 7.4 [8] and 7.6 (D.L.H., unpublished data, 1999) and the slower differentiation of granulocytic cells at these pH values relative to pH 7.25. Modulation of G-CSFR expression and differentiation by pH, but not by pO_2 , support the model's finding for independent mechanisms of pH and pO_2 regulation.

Simulations of data obtained from $-IL-3$ vs $+IL-3$ experiments were used to delineate the specific modes of action of IL-3, out of its broad repertoire [9–13,48,49], that regulate granulopoiesis in the cultures under examination. The lack of enhancement in the transition rate out of quiescence with the addition of IL-3, as illustrated by an unchanging α , indicated that the presence of SCF, G-CSF, and IL-6 was a sufficient stimulus to induce cycling. This is consistent with reports that IL-3 exerts its influence on cells only after they have left quiescence [50]. Other studies reporting IL-3's anti-apoptotic benefits led us to expect an increased death rate of early progenitors in the absence of IL-3. However, modeling of the experimental results shows only a slightly elevated death rate for cells in early stages of differentiation. The presence of saturating amounts of SCF and G-CSF, two cytokines with well-known anti-apoptotic

properties [12,51–54], likely compensated for the lack of IL-3 in this regard. Hence, the model revealed that the major effect of IL-3 in these cultures was to regulate growth and differentiation. Even more significant, from a mechanistic point of view, is that this regulation is variable with maturation stage.

Given that every cell of a specific population requires a certain minimum cycling time to divide, differentiation rates that are too fast could lead to skipped cell divisions. Acceleration of the differentiation rate through the myeloblast stage ($0.46 < \tau < 0.56$) likely resulted in skipped divisions, which then translated to less cell expansion in $-IL-3$ cultures. Through model analysis, it was determined that myeloblast cells, which are at an intermediate stage of differentiation, are more sensitive to IL-3 than are more mature postprogenitors or the more primitive CFU-G. Interestingly, the rapid increase in levels of G-CSFR on the cell surface coincides with this stage (D.L.H., unpublished data, 1999). An antagonistic action of IL-3 on G-CSFR-mediated differentiation is suggested by accelerated G-CSFR expression and differentiation kinetics in our cultures that lack IL-3. There are several reports that IL-3 may offset the effects of G-CSF on granulocytic differentiation [55–59]. Thus, the enhanced differentiation rate of cells through the myeloblast stage in $-IL-3$ cultures could be due to an uninhibited granulocytic differentiation signal.

In examining the potential interactions between pH and pO_2 or between pH and IL-3, the unanticipated additive nature of the individual pO_2 -, pH-, or IL-3-associated changes in the model parameters allowed for the prediction of culture behavior. We were able to conclude from this interesting finding that pO_2 and IL-3 each regulates granulopoiesis through pathways distinct from pH.

The simplicity, flexibility, and predictive power of the model when confronted by a wide variety of experimental conditions make it a valuable tool in defining possible mechanisms of inefficient granulopoiesis. Although it is possible that similar agreement between simulation and data could be obtained using other combinations of model parameters for each condition, the approach taken here of changing a minimum number of parameters and applying these changes across the entire range of τ —except as supported by experimental evidence or physiologic data—increases the confidence that our model results captured the underlying phenomena. This model can be applied to other situations that alter growth and differentiation, extending beyond pH, pO_2 , and IL-3. In particular, this model has important implications in studying possible pathophysiologic mechanisms underlying perturbations of granulopoiesis in leukemic cells. Furthermore, the insight gained through use of this model could help improve strategies for the *ex vivo* production of granulocytic precursors—the transplantation of which has been suggested to possibly lead to a shortening or even abrogation of neutropenia following high-dose chemotherapy [17–21]. The characterization of the granulocytic branch of

hematopoiesis also is an important step toward ultimately being able to predict complex multilineage kinetics based on known initial conditions and environmental parameters.

Acknowledgments

Supported by grant BES-9809730 from the National Science Foundation and grant R01 HL48276 from the National Institutes of Health. D.L.H. was supported in part by carcinogenesis training grant CA09560 from the National Institutes of Health. We thank Amgen for donation of stem cell factor. We are grateful to Response Oncology (especially Chet Cudak, Cathy Allen, and Dr. Bonnie Hazelton) for providing apheresis products. We also would like to thank Dr. Lars Nielsen of the University of Queensland, Brisbane, Australia, for valuable discussions.

References

1. Terstappen LW, Safford M, Loken MR (1990) Flow cytometric analysis of human bone marrow. III. Neutrophil maturation. *Leukemia* 4:657
2. Jandl JH (1996) *Blood*. Textbook of Hematology. Boston: Little, Brown and Company
3. Koller MR, Bender JG, Miller WM, Papoutsakis ET (1992) Reduced oxygen tension increases hematopoiesis in long-term culture of human stem and progenitor cells from cord blood and bone marrow. *Exp Hematol* 20:264
4. Koller MR, Bender JG, Papoutsakis ET, Miller WM (1992) Effects of synergistic cytokine combinations, low oxygen, and irradiated stroma on the expansion of human cord blood progenitors. *Blood* 80:403
5. Laluppa JA, Papoutsakis ET, Miller WM (1998) Oxygen tension alters the effects of cytokines on the megakaryocyte, erythrocyte, and granulocyte lineages. *Exp Hematol* 26:835
6. McAdams TA, Miller WM, Papoutsakis ET (1997) Variations in culture pH affect the cloning efficiency and differentiation of progenitor cells in ex vivo haemopoiesis. *Br J Haematol* 97:889
7. McAdams TA, Miller WM, Papoutsakis ET (1998) pH is a potent modulator of erythroid differentiation. *Br J Haematol* 103:317
8. Hevehan DL, Papoutsakis ET, Miller WM (2000) Physiologically significant effects of pH and oxygen tension on granulopoiesis. *Exp Hematol* 28:267
9. Iscove NN, Shaw AR, Keller G (1989) Net increase of pluripotential hematopoietic precursors in suspension culture in response to IL-1 and IL-3. *J Immunol* 142:2332
10. Metcalf D (1991) Lineage commitment of hemopoietic progenitor cells in developing blast cell colonies: influence of colony-stimulating factors. *Proc Natl Acad Sci U S A* 88:11310
11. Kelvin DJ, Chance S, Shreeve M, Axelrad AA, Connolly JA, McLeod D (1986) Interleukin 3 and cell cycle progression. *J Cell Physiol* 127:403
12. Brandt JE, Bhalla K, Hoffman R (1994) Effects of interleukin-3 and c-kit ligand on the survival of various classes of human hematopoietic progenitor cells. *Blood* 83:1507
13. Clark SC, Kamen R (1987) The human hematopoietic colony-stimulating factors. *Science* 236:1229
14. Loeffler M, Wichmann HE (1985) Structure of the model. In: Loeffler M, Wichmann HE (eds.) *Mathematical modeling of cell proliferation: stem cell regulation in hemopoiesis*. Boca Raton: CRC Press, p. 55
15. Schmitz S, Franke H, Brusis J, Wichmann HE (1993) Quantification of the cell kinetic effects of G-CSF using a model of human granulopoiesis. *Exp Hematol* 21:755
16. Nielsen LK, Papoutsakis ET, Miller WM (1998) Modelling ex vivo hematopoiesis using chemical engineering metaphors. *Chem Eng Sci* 53:1913
17. Williams SF, Lee WJ, Bender JG, et al. (1996) Selection and expansion of peripheral blood CD34⁺ cells in autologous stem cell transplantation for breast cancer. *Blood* 87:1687
18. Brugger W, Heimfeld S, Berenson RJ, Mertelsmann R, Kanz L (1995) Reconstitution of hematopoiesis after high-dose chemotherapy by autologous progenitor cells generated ex vivo. *N Engl J Med* 333:283
19. Reiffers J, Calliot C, Dazey B, Attal M, Caraux J, Boiron JM (1999) Abrogation of post-myeloablative chemotherapy neutropenia by ex vivo expanded autologous CD34-positive cells. *Lancet* 354:1092
20. Nielsen LK, Bender JG, Miller WM, Papoutsakis ET (1998) Population balance model of in vivo neutrophil formation following bone marrow rescue therapy. *Cytotechnology* 28:157
21. Scheding S, Franke H, Diehl V, et al. (1999) How many myeloid post-progenitor cells have to be transplanted to completely abrogate neutropenia after peripheral blood progenitor cell transplantation? Results of a computer simulation. *Exp Hematol* 27:956
22. Cronkite EP, Vincent PC (1969) Granulocytopoiesis. *Ser Haemat* 4:3
23. Mayani H, Lansdorp PM (1995) Proliferation of individual hematopoietic progenitors purified from umbilical cord blood. *Exp Hematol* 23:1453
24. Schiesser WE (1994) *Computational mathematics in engineering and applied science: ODEs, DAEs, and PFEs*. Boca Raton: CRC Press
25. Civin CI, Loken MR (1987) Cell surface antigens on human marrow cells: dissection of hematopoietic development using monoclonal antibodies and multiparameter flow cytometry. *Int J Cell Cloning* 5:267
26. Lu L, Xiao M, Shen R-N, Grigsby S, Broxmeyer HE (1993) Enrichment, characterization, and responsiveness of single primitive CD34⁺⁺⁺ human umbilical cord blood hematopoietic progenitors with high proliferative and replating potential. *Blood* 81:41
27. Lu L, Xiao M, Grigsby S, et al. (1993) Comparative effects of suppressive cytokines on isolated single CD34⁺⁺⁺ stem/progenitor cells from human bone marrow and umbilical cord blood plated with and without serum. *Exp Hematol* 21:1442
28. Huang S, Law P, Young D, Ho AD (1998) Candidate hematopoietic stem cells from fetal tissues, umbilical cord blood vs. adult bone marrow and mobilized peripheral blood. *Exp Hematol* 26:1162
29. Huang S, Chen Z, Yu JF, et al. (1999) Correlation between IL-3 receptor expression and growth potential of human CD34⁺ hematopoietic cells from different tissues. *Stem Cells* 17:265
30. Cronkite EP, Fliedner TM (1964) Granulocytopoiesis. *N Engl J Med* 270:1347
31. Smeby W, Benestad HB (1980) Simulation of murine granulopoiesis. *Blut* 41:47
32. Young JC, DiGiusto D, Backer MP (1996) In vitro characterization of fetal hematopoietic stem cells: range and kinetics of cell production from individual stem cells. *Biotech Bioeng* 50:465
33. Makino S, Haylock DN, Douse T, et al. (1997) Ex vivo culture of peripheral blood CD34⁺ cells: effects of hematopoietic growth factors on production of neutrophilic precursors. *J Hematother* 6:475
34. Martinson JA, Unverzagt K, Schaeffer A, et al. (1998) Neutrophil precursor generation: effects of culture conditions. *J Hematother* 7:463
35. Maritz JS, Stanley ER, Yeo GF, Metcalf C (1972) A model of hematopoietic cell colony formation. *Biometrics* 28:801
36. Roti JL, Okada S (1973) A mathematical model of cell cycle of L5178Y. *Cell Tissue Kinet* 6:111
37. Francis GE, Leaning MS (1985) Stochastic model of human granulocyte-macrophage progenitor cell proliferation and differentiation. I. Setting up the model. *Exp Hematol* 13:92
38. Koller MR, Bender JG, Papoutsakis ET, Miller WM (1992) Beneficial effects of reduced oxygen tension and perfusion in long-term hematopoietic cultures. *Ann N Y Acad Sci* 665:105
39. Smith S, Broxmeyer HE (1986) The influence of oxygen tension on the long-term growth in vitro of hematopoietic progenitor cells from human cord blood. *Br J Haematol* 63:29
40. Ishikawa Y, Ito T (1988) Kinetics of hemopoietic stem cells in a hypoxic culture. *Eur J Haematol* 40:126
41. Bradley TR (1978) The effect of oxygen tension on hematopoietic and fibroblastic cell proliferation in vitro. *J Cell Physiol* 97:517

42. Rich IN, Kubanek B (1982) The effect of reduced oxygen tension on colony formation of erythropoietic cells in vitro. *Br J Haematol* 52:579
43. Broxmeyer HE, Cooper S, Gabig T (1989) The effects of oxidizing species derived from molecular oxygen on the proliferation in vitro of human granulocyte-macrophage progenitor cells. *Ann N Y Acad Sci* 554:177
44. Clerch LB, Massaro DJ (1997) Oxygen, gene expression, and cellular function. New York: Marcel Dekker
45. Avalos BR (1996) Molecular analysis of the granulocyte colony-stimulating factor receptor. *Blood* 88:761
46. Demetri GD, Griffin JD (1991) Granulocyte colony-stimulating-factor and its receptor. *Blood* 78:2791
47. Fliedner TM, Hoelzer D, Steinbach KH (1982) Blast cell and granulocyte production in human leukemia: pathophysiological concepts based on computer simulation using discrete modeling techniques. *Blood Cells* 8:535
48. Sato N, Sawada K, Koizumi K, et al. (1993) In vitro expansion of human peripheral blood CD34+ cells. *Blood* 82:3600
49. Caux C, Favre C, Saeland S, et al. (1989) Sequential loss of CD34 and class II MHC antigens on purified cord blood hematopoietic progenitors cultured with IL-3: characterization of CD34⁻, HLA⁻DR⁺ cells. *Blood* 74:1287
50. Ogawa M (1993) Differentiation and proliferation of hematopoietic stem cells. *Blood* 81:2844
51. Migliaccio G, Migliaccio AR, Druzin ML, Giardina PJ, Zsebo KM, Adamson JW (1992) Long-term generation of colony-forming cells in liquid culture of CD34+ cord blood cells in the presence of recombinant human stem cell factor. *Blood* 79:2620
52. Leary AG, Zeng HQ, Clark SC, Ogawa M (1992) Growth factor requirements for survival in G₀ and entry into the cell cycle of primitive human hemopoietic progenitors. *Proc Natl Acad Sci U S A* 89:4013
53. Philpott NJ, Prue RL, Marsh JC, Gordon-Smith EC, Gibson FM (1997) G-CSF-mobilized CD34⁺ peripheral blood stem cells are significantly less apoptotic than unstimulated peripheral blood CD34⁺ cells: role of G-CSF as survival factor. *Br J Haematol* 97:146
54. Itoh Y, Ikebuchi K, Hirashima K (1992) Interleukin-3 and granulocyte colony-stimulating factor as survival factors in murine hemopoietic stem cells in vitro. *Int J Hematol* 55:139
55. Walker F, Nicola NA, Metcalf D, Burgess AW (1985) Hierarchical down-modulation of hemopoietic growth factor receptors. *Cell* 43:269
56. Valtieri M, Twardy DJ, Caracciolo D, et al. (1987) Cytokine-dependent granulocytic differentiation: regulation of proliferative and differentiative responses in a murine progenitor cell line. *J Immunol* 138:3829
57. Fukunaga R, Ishizaka-Ikeda E, Nagata S (1993) Growth and differentiation signals mediated by different regions in the cytoplasmic domain of granulocyte colony-stimulating factor receptor. *Cell* 74:1079
58. Steinman RA, Twardy DJ (1994) Granulocyte colony-stimulating factor receptor mRNA upregulation is an immediate early marker of myeloid differentiation and exhibits dysfunctional regulation in leukemic cells. *Blood* 83:119
59. Steinman RA, Iro A (1999) Suppression of G-CSF-mediated Stat signalling by IL-3. *Leukemia* 13:54

Appendix

A-1. Initial cell distribution

On day 0, given a mean viability of 80%, an adjusted total cloning efficiency of 55% (see Parameter estimation), and the measured % CFU-G/CFC equal to an average of 42%, cultures that were inoculated at 2×10^4 total CD34⁺ cells/mL effectively contained $\sim 3,719$ granulocytic cells/mL (range 2,928 to 4,081 cells/mL, $n = 6$). Under control

conditions, these cells underwent an average of 12.8 divisions. A β distribution is used to describe the initial cell population distributed over a range of differentiation values from 0 to 1 [16] (A.1):

$$f(\tau; a, b) = \frac{1}{B(a, b)} \tau^{a-1} (1-\tau)^{b-1}; \quad 0 < \tau < 1 \quad (\text{A.1})$$

where $B(a, b)$ is the beta function with $a = 6.9$ and $b = 20$. The two constants, a and b , were calculated based on the following two experimental observations. First, for cells initially located at $\tau = 0$, the maximum number of divisions is 17 [23]. Thus, cells initially located between $0 < \tau < 0.87$ would be capable of $17(1 - \tau/0.87)$ divisions, whereas cells at $0.87 < \tau < 1$ would be capable of 0 divisions due to their nonproliferative state. Because the average observed total cell expansion was equal to $2^{12.8}$, it follows (A.2):

$$\int_{\tau=0}^1 f(\tau) 2^{17\left(1 - \frac{\tau}{0.87}\right)} d\tau = 2^{12.8}. \quad (\text{A.2})$$

Second, because 100% of initial granulocytic cells were CFU-G, we have (A.3):

$$\int_{\tau=0}^{0.56} f(\tau) d\tau = 1. \quad (\text{A.3})$$

Assuming that all cells are quiescent at the onset of culture, i.e., that $n(0, \tau) = 0$ and $N_M(0) = 0$, the initial distribution takes the form (A.4):

$$n_0(0, \tau) = N_T(0)f(\tau) \quad (\text{A.4})$$

where $N_T(0) = 3,719$ as described earlier.

In our cultures, an average of 12.8 divisions, with a theoretical potential for 17 divisions from the most primitive CFU-G stage, translates to an average initial $\tau = 0.24$. Thus, the initial distribution of cells in our system was characteristic of a more committed state. This is consistent with the starting population of CD34⁺CD45RA^{low}CD71^{low} cord blood cells used by Mayani and Lansdorp [23] that was highly enriched for primitive hematopoietic progenitor cells, including long-term culture initiating cells, high-proliferative potential-CFC, and CFU-Mix, vs our starting population of peripheral blood CD34⁺ cells that was not further purified and consisted mostly of CFU-G, CFU-M, and burst-forming unit erythroid. Rare multipotent progenitors, CFU-Mix and CFU-GM, were assumed to give rise to granulocytic cells, especially in the presence of granulopoietic-promoting cytokines, and were included in the immature CFU-G population. With essentially no cells at $\tau = 0$, even at $t = 0$, the following boundary condition can be applied to solve Equations 1–3 (A.5):

$$n(t, 0) = 0; \quad t > 0. \quad (\text{A.5})$$

A-2. Observed granulocytic cell types and their weighting functions

Weighting functions are needed to relate model outputs to observed quantities. A weighting function, which indicates the probability that a cell at differentiation stage τ will score in a particular population, is assigned to each differentiation marker. The probabilities reflect the ordered progression of granulocytic differentiation, with cells first becoming CD15⁺, then CD15^{bright}, and finally CD11b⁺. The three weighting functions take the form of a general logistic function [16] (A.6–A.8):

$$w_{\text{CD15}^+}(\tau) = \frac{1}{1 + e^{-\frac{\tau - p_1}{s_1}}}; \quad (\text{A.6})$$

$$p_1 = 0.32 \text{ and } s_1 = -0.05$$

$$w_{\text{CD15}^{\text{bright}}}(\tau) = w_{\text{CD15}^+}(\tau) \frac{1}{1 + e^{-\frac{\tau - p_2}{s_2}}};$$

$$p_2 = 0.42 \text{ and } s_2 = -0.10 \quad (\text{A.7})$$

$$w_{\text{CD11b}^+}(\tau) = w_{\text{CD15}^{\text{bright}}}(\tau) \frac{1}{1 + e^{-\frac{\tau - p_3}{s_3}}};$$

$$p_3 = 0.75 \text{ and } s_3 = -0.067 \quad (\text{A.8})$$

with the constants p and s chosen such that the model closely fits the observed number of relevantly stained cells as a function of time under control conditions. With the indicated p and s values, $w_{\text{CD15}^+}(\tau)$, $w_{\text{CD15}^{\text{bright}}}(\tau)$, and $w_{\text{CD11b}^+}(\tau)$ increase from zero at $\tau = 0$ and approach one for $\tau > 0.46$, $\tau > 0.56$, and $\tau > 0.77$, respectively.

Initially, all cells are quiescent and do not express CD15 or CD11b. Because cells do not revert back into quiescence ($\beta = 0$) once they start to differentiate and acquire these surface antigens, we assume that quiescent cells will not be CD15⁺ or CD11b⁺, i.e., $w_0 = 0$. Furthermore, any mature neutrophils will score positive for CD15 and CD11b, i.e., $w_M = 1$. Hence, the relationships for each cell population are given by (see Equation 4) (A.9–A.11):

$$O_{\text{CD15}^+}(t) = \int_{\tau=0}^1 w_{\text{CD15}^+}(\tau) n(t, \tau) d\tau + N_M(t) \quad (\text{A.9})$$

$$O_{\text{CD15}^{\text{bright}}}(t) = \int_{\tau=0}^1 w_{\text{CD15}^{\text{bright}}}(\tau) n(t, \tau) d\tau + N_M(t) \quad (\text{A.10})$$

$$O_{\text{CD11b}^+}(t) = \int_{\tau=0}^1 w_{\text{CD11b}^+}(\tau) n(t, \tau) d\tau + N_M(t). \quad (\text{A.11})$$

For total viable cells, where all weights are equal to 1, Equation 4 reduces to (A.12):

$$N_T(t) = \int_{\tau=0}^1 (n_0(t, \tau) + n(t, \tau)) d\tau + N_M(t). \quad (\text{A.12})$$